The Phanerozoic diversification of silica-cycling testate amoebae and its possible links to changes in terrestrial ecosystems

Daniel J. G. Lahr, Tanja Bosak, Enrique Lara, Edward A. D. Mitchell

The terrestrial cycling of Si is thought to have a large influence on the terrestrial and marine primary production, as well as the coupled biogeochemical cycles of Si and C. Biomineralization of silica is widespread among terrestrial eukaryotes such as plants, soil diatoms, freshwater sponges, silicifying flagellates and testate amoebae. Two major groups of testate (shelled) amoebae, arcellinids and euglyphids, produce their own silica particles to construct shells. The two are unrelated phylogenetically and acquired biomineralizing capabilities independently. Hyalosphenids, a group within arcellinids, are predators of euglyphids. We demonstrate that hyalosphenids can construct shells using silica scales mineralized by the euglyphids. Parsimony analyses of the current hyalosphenid phylogeny indicate that the ability to “steal” euglyphid scales is most likely ancestral in hyalosphenids, implying that euglyphids should be older than hyalosphenids. However, exactly when euglyphids arose is uncertain. Current fossil record contains unambiguous euglyphid fossils that are as old as 50 million years, but older fossils are scarce and difficult to interpret. Poor taxon sampling of euglyphids has also prevented the development of molecular clocks. Here, we present a novel molecular clock reconstruction for arcellinids and consider the uncertainties due to various previously used calibration points. The new molecular clock puts the origin of hyalosphenids in the early Carboniferous (~370 mya). Notably, this estimate coincides with the widespread colonization of land by Si-accumulating plants, suggesting possible links between the evolution of Arcellinid testate amoebae and the expansion of terrestrial habitats rich in organic matter and bioavailable Si.

Title: The Phanerozoic diversification of silica-cycling testate amoebae and its possible links to changes in terrestrial ecosystems

Manuscript submitted to *peerJ* as **Research Article**

Authors: Daniel J. G. Lahr[1], Tanja Bosak[2], Enrique Lara[3] and Edward A. D. Mitchell[3,4]

Running Title: Silica biomineralization in early eukaryotes

Affiliations:

1 – Dept. of Zoology, Institute of Biosciences, University of São Paulo, Rua do Matão, travessa 14, São Paulo, Brazil

2 – Department of Earth, Atmospheric and Planetary Sciences, Massachusetts Institute of Technology, 77 Massachusetts Avenue, E25-649, Cambridge, MA 02139

3 – Laboratory of Soil Biology, University of Neuchatel, Rue Emile Argand 11, CH-2000 Neuchatel, Switzerland

4 – Jardin Botanique de Neuchâtel, Chemin du Perthuis-du-Sault 58, CH-2000 Neuchâtel, Switzerland

Corresponding author: Daniel J. G. Lahr dlahr@ib.usp.br , Phone: +55 (11) 30910948, Fax +55(11)30917513

ABSTRACT The terrestrial cycling of Si is thought to have a large influence on the terrestrial and marine primary production, as well as the coupled biogeochemical cycles of Si and C. Biomineralization of silica is widespread among terrestrial eukaryotes such as plants, soil diatoms, freshwater sponges, silicifying flagellates and testate amoebae. Two major groups of testate (shelled) amoebae, arcellinids and euglyphids, produce their own silica particles to construct shells. The two are unrelated phylogenetically and acquired biomineralizing capabilities independently. Hyalosphenids, a group within arcellinids, are predators of euglyphids. We demonstrate that hyalosphenids can construct shells using silica scales mineralized by the euglyphids. Parsimony analyses of the current hyalosphenid phylogeny indicate that the ability to “steal” euglyphid scales is most likely ancestral in hyalosphenids, implying that euglyphids should be older than hyalosphenids. However, exactly when euglyphids arose is uncertain. Current fossil record contains unambiguous euglyphid fossils that are as old as 50 million years, but older fossils are scarce and difficult to interpret. Poor taxon sampling of euglyphids has also prevented the development of molecular clocks. Here, we present a novel molecular clock reconstruction for arcellinids and consider the uncertainties due to various previously used calibration points. The new molecular clock puts the origin of hyalosphenids in the early Carboniferous (~370 mya). Notably, this estimate coincides with the widespread colonization of land by Si-accumulating plants, suggesting possible links between the evolution of Arcellinid testate amoebae and the expansion of terrestrial habitats rich in organic matter and bioavailable Si.

Key Words: Microbial eukaryote evolution, silica biomineralization, silica cycle, molecular dating, carbon and silica cycles link

Introduction

Si is a major rock-forming element with a cycle that influences the growth of primary producers and carbon burial in the oceans (Sarmiento, 2013). Over geological time scales, the biogeochemical cycles of carbon and silica are linked through the weathering of continents, which dissolves Si from rocks and delivers it to the oceans (Wilkinson & Mitchell, 2010). On shorter time scales, Si cycles vigorously in soils and forms a soil pool that is 2-3 orders of magnitude larger than the Si pool in living terrestrial biomass (Cornelis et al., 2011). Thus, plant-microbe-mineral interactions that control this sizeable pool of soil Si ultimately control the availability of dissolved Si and the delivery of Si to the oceans (Conley, 2002). Plants are thought to be the major contributors to the terrestrial cycling of Si because they can promote the weathering of rocks, accumulate Si from the soil solution and biomineralize amorphous Si in the form of phytoliths (Alexandre et al., 1997; Cornelis et al., 2011). Phytoliths released from dead plant matter can form a pool with a lower turnover rate relative to other forms of biogenic silica (Alexandre et al., 1997). This pool comprises more than 90% of biogenic Si delivered to rivers (Cary et al., 2005) and is the main source of reactive Si in soils. Research in the past three decades has revealed much about the role of plant-derived biogenic Si in the terrestrial cycling of Si (Conley, 2002). In contrast, the contribution and the long term history of Si-biomineralizing microbial groups in terrestrial ecosystems are less well understood (Wilkinson & Mitchell, 2010). Many microbial eukaryotes use silica to build external and internal skeletons, and have molecular mechanisms for Si uptake. Up to 77 genes regulated by silicic acid in the diatom *Phaeodactylum tricornutum* have orthologs in the genomes of other eukaryotes, including Opisthokonts, Viridiplantae and other “Chromalveolates” (~~(~~Sapriel et al., 2009~~)~~; see also **Figure 1**). The genes implicated in silica metabolism may have been exchanged among eukaryotic clades through lateral gene transfer, as demonstrated for choanoflagellates and diatoms (Marron et al., 2013). In terrestrial systems, testate amoebae (i.e. amoebae that construct shells)

are among the most abundant and conspicuous organisms that use silica. The existing studies show that: 1) testate amoebae can contribute up to 10% of biogenic silica in some tropical soils and rivers (Cary et al., 2005); and 2) the annual incorporation of Si by testate amoebae can in some cases match the amounts of Si released by plant phytoliths (Aoki, Hoshino & Matsubara, 2007; Wilkinson, 2008; M. Sommer, 2012; Puppe et al., 2014). These observations, as well as the long evolutionary history of testate amoebae (Lahr, Grant & Katz, 2013), suggest a role for testate amoebae in the terrestrial silica cycle and motivate this study.

There are several groups of unrelated testate amoebae. The two most prevalent and abundant in terrestrial environments are the euglyphid and the arcellinid testate amoebae. Both inhabit the same environments –bodies of fresh water, soils, peatlands and other humid microhabitats – and have approximately the same sizes, with the majority of species being between 30-300 μm long or wide. However, the two groups are vastly divergent genetically and historically. Euglyphids include about 800 species and are in the super group Rhizaria (**Figure 1**). These organisms produce thin, pointed, non-anastomosed pseudopods and almost all extant lineages in the group are silica biomineralizers. Thus, biomineralization is likely ancestral in the group. Owing to the preservation of siliceous shells, euglyphids have a ~~fossil~~ record that goes ~~back~~ 30-50 million years (Foissner & Schiller, 2001; Barber, Siver & Karis, 2013). The arcellinid testate amoebae encompass about 2000 species and are in the super group Amoebozoa (**Figure 1)**. These amoebae produce rounded, blunt pseudopods and have a great diversity of shell compositions – organic, agglutinated and biomineralized. The fossil record of arcellinids is much older than that of euglyphids, and there is consensus that some vase shaped microfossils dating back to the Neoproterozoic (ca. 750 mya) belong to the arcellinids (Porter & Knoll, 2009; Bosak et al., 2011; Lahr, Grant & Katz, 2013; Strauss et al., 2014).

Biomineralization of silica in testate amoebae occurs in many different ways. The shell

is always constructed shortly before cell division: a new shell is produced through the aperture of the older shell. After cell division, one daughter cell stays in the old shell and the other daughter cell inherits the new shell (Hedley & Ogden, 1974). Most euglyphids produce silica scales in the cytoplasm, presumably taking up dissolved Si and depositing it as amorphous silica *via* silica deposition vesicles (Hedley & Ogden, 1974; Anderson, 1994; Gröger, Lutz & Brunner, 2008). The scales, which are typically shorter than 10μm and thinner than 2μm, are then used as building blocks to construct the shell. The specific literature refers to these types of building blocks produced by testate amoebae as *idiosomes*. A small number of arcellinids use a similar strategy – *Lesquereusia*, *Netzelia,* and especially *Quadrulella* (**Figure 2A**) are three genera known to produce silica idiosomes (Anderson, 1987, 1989, 1994; Meisterfeld, 2002). *Netzelia* is able to precipitate idiosomes, but is also known to deposit silica around ingested particles, including starch and various minerals, and then use these particles to build the daughter shell (Anderson, 1987, 1989). *Quadrulella*, on the other hand, produces its shell entirely of square siliceous idiosomes. Many arcellinids use siliceous particles and mineral grains scavenged from the environment as unmodified building blocks named *xenosomes* [*Difflugia* (**Figure 2B**) and *Heleopera* are well-known examples (Meisterfeld, 2002; Châtelet, Noiriel & Delaine, 2013)]. Others are able to lightly modify siliceous particles either by dissolution or deposition (e.g. *Nebela* (**Figure 2C**) and related genera [*Padaungiella, Argynnia* (**Figure 2D**)], as well as the *insertae sedis Lesquereusia* (Anderson, 1987, 1989).

Both classical and modern studies report the usage of euglyphid scales by arcellinid amoebae of the Hyalospheniidae family (Leidy, 1879; Penard, 1902; Deflandre, 1936; Douglas & Smol, 2001; Meisterfeld, 2002). These amoebae reportedly obtain silica plates by preying on euglyphids, and then use the stolen scales to build the shell (Deflandre, 1936) – a phenomenon we name *kleptosquamy* (Figure 3). Here, we record several stages of this phenomenon in *Padaungiella lageniformis* that preys upon *Euglypha* sp. Next, we ask whether *kleptosquamy* is

ancestral in the hyalosphenid testate amoebae and use this to determine the order in which hyalosphenids and euglyphids emerged. To better time the rise of biomineralization in hyalosphenids, we also provide a novel molecular clock reconstruction of the arcellinids. Finally, we discuss the implications of the revised molecular clock in light of broader evolutionary and biogeochemical trends.

Material & Methods

Microscopical observations

Samples of *Sphagnum* sp. were collected in *Les Pontins* peat bog in Canton Bern, Switzerland (47° 7'39.11"N; 6°59'27.35"E). Microscopic observations were made using an Utermöhl chamber (Cat #435025, HydroBios, Germany) on an Olympus IX81 inverted microscope equipped with oil immersion Differential Interference Contrast optics (20x-40x-60x-100x). All images were recorded by an Olympus DP-71 camera.

Ancestral state reconstructions

We have performed ancestral state reconstructions on the topologies from molecular reconstructions of two recently published phylogenies (Kosakyan et al., 2012; Oliverio et al., 2014). Each reconstruction is based on a distinct set of molecular data (Cox1 and SSU rDNA respectively). Ancestral state reconstruction was performed in the program Mesquite (Maddison & Maddison, 2007) using parsimony as an optimality criterion, for the single character *kleptosquamy*, with possible states present, absent or unknown.

Molecular clock reconstructions

Molecular clock reconstructions (MCR) were performed using PhyloBayes 3.3 (Lartillot, Lepage & Blanquart, 2009). We used the final tree and alignment for SSU rDNA small subunit

ribosomal gene published by ~~Lahr et al. (Lahr, Grant & Katz, 2013)~~ as a tree onto which we calculated divergence times. Calibration points were the 6 opisthokont fossils also used by Parfrey et al. (Parfrey et al., 2011), whereas the Arcellinida calibration point is based on the fossil *Paleoarcella athanata* (type specimen HUPC #62988), described in Porter et al. (2003). The dating of ~~sediment~~ for this fossil was an ash bed 2 meters above the fossils, calculated by U-Pb zircon chronology (Karlstrom et al., 2000) (Table 1). The opisthokont fossils used by ~~(Parfrey et al., 2011)~~ are congruent with those proposed and justified for animals by ~~(Benton et al., 2015)~~ With additional data present in current tree, it was possible to use the Chuar group fossils as a calibration point for the actual last common ancestor of arcellinids (Porter & Knoll, 2000), rather than the divergence between arcellinids and other naked amoebae, as in Parfrey and colleagues (2011). One alternative run was also generated incorporating the three additional Meso- and Cenozoic fossils as calibration points within the Arcellinida, as suggested by ~~Fiz-Palacios et al. (Fiz-Palacios, Leander & Heger, 2014)~~: origin of the *Centropyxis* genus [termed “node B” in Fiz-Palacios et al. (2014)] was set to the split between *Hyalosphenia papilio* and *Arcella hemisphaerica*, with lower and upper bounds at 736-220 mya, origin of hyalosphenids (“node C”) was set to the split between *Padaungiella lageniformis* and *Hyalosphenia elegans* with soft bounds at 736-100mya; origin of genus *Arcella* (“node D”), calibrated the clade containing *A. hemisphaerica* and *A. vulgaris* WP with soft bounds at 105-100mya. We did not include the fourth calibration point suggested by Fiz-Palacios and colleagues (*Lesquereusia* – *Difflugia* divergence) because the *Lesquereusia* SSU rDNA is not available. Fortunately, Fiz-Palacios and colleagues have tested their dataset for sensitivity to this particular calibration point and have determined that its inclusion does not significantly modify the final result (Fiz-Palacios, Leander & Heger, 2014). We have performed MCRs by running two independent chains with a burn-in factor of 100 until the effective size of samples was above 50 and the maximum discrepancy between chains was below 0.3. These parameters are suggested as values for an “acceptable run” by the PhyloBayes manual. We used soft

constraints on the calibration dates to account for uncertainty in the fossil dates as advocated by several researchers (~~Donoghue~~ & Benton, 2007; Parfrey et al., 2011). The use of soft constraints requires a model of birth-death for the prior on divergence times. We performed reconstructions using both the GTR and the CAT-GTR models for nucleotide substitutions. We have performed MCR using three distinct models for rate distributions: two auto correlated models (CIR and lognormal) as well as the uncorrelated gamma multipliers model. We performed comparisons for model fit by computing Bayes Factors by thermodynamic integration under the normal approximation, as discussed in Phylobayes 3.3 manual, and recommended in Lartillot and Phillipe (2006). In order to do so, a variance-covariance matrix was obtained using the program *estbranches* [part of *multdivtime* package (Thorne & Kishino, 2003)], with input parameters calculated in *baseml* [part of the PAML package (Yang, 2007)], following instructions by Rutschmann (2005).

Results

Microscopical observations

An individual *Padaungiella lageniformis* was isolated while preying upon a specimen of *Euglypha* sp. The *Euglypha* cytoplasm had been almost completely ingested at the stage of isolation (**Figure 3A, B, C**). We observed the *P. lageniformis* removing and ingesting siliceous plates from the prey organism's shell for around 10 minutes (**Figure 3D**). Immediately afterwards, the individual deposited siliceous plates in the inner part of the “neck” of its shell, parallel to the aperture (**Figure 3E**) and moved large cytoplasmic debris in the same direction (**Figure 3E,F**). The organism was constructing a plug in the aperture, which became visible at the end of this activity that lasted for approximately one hour. There was no indication that any of the plates were dissolved in the cytoplasm: all previously ingested plates were kept intact and moved towards the aperture. After one hour, the amoeba added multiple additional layers to the

previously laid down barrier (**Figures 3G, H, I**). Though the scales formed most of the barrier, other types of debris were added as well. After about two hours of actively plugging the aperture, the amoeba encysted, presumably with digestive function (**Figures 3J, K**). The amoeba remained encysted for at least two more hours. Resumed observations approximately 12 hours later revealed that the amoeba had emerged from the digestive cyst and re-ingested all siliceous plates (Figure L). However, the organism had discarded the yellowish-brown types of debris (**Figure 3L**). The siliceous plates did not appear to be separated from any other cytoplasmic structures by membranes. Many gathered around the nucleus at times. Two days after the initial ingestion, the amoeba went into a second resting cyst (it is relevant to note that the amoeba was maintained in an environmental sample and had access to ample food items), where it remained for over 24 hours, but did not exhibit other relevant changes. We discontinued observations approximately 80 hours after initial observation (4 days).

Ancestrality of kleptosquamy

Observations of kleptosquamy and the associated behavioral attitudes enable evolutionary interpretations in other closely related hyalosphenid testate amoebae. The conspicuous plug made of scales created by *Padaungiella*, as well as the presence of modified euglyphid scales in the shell is observed in most other hyalosphenids, including the genera: *Apodera, Certesella* (Meisterfeld, 2002), *Porosia* (**Figure 4A**), and finally *Nebela* (**Figure 4B**). One other genus has shells that contain small, possibly siliceous scales with undetermined origin: *Physochila* and *Argynnia* (**Figure 2D,** (Vucetich, 1974)) were shown not to be closely related to hyalosphenids (Gomaa et al., 2012). Considering the most current molecular data available, *Padaungiella* is a basal lineage (Lara et al., 2008; Heger et al., 2011; Gomaa et al., 2012; Kosakyan et al., 2012; Lahr, Grant & Katz, 2013). Other four genera (*Apodera, Certesella,*

Porosia, Nebela) are able to re-use scales obtained from euglyphids and three others (*Quadrulella*, *Hyalosphenia* and *Alocodera*) do not . We have performed a parsimony based ancestral reconstruction of character states in both topologies available (based on mitochondrial and nuclear genes, **Figure 5**). Under any of the two scenarios scenario, kleptosquamy appears in the ancestral hyalosphenid, and is lost twice: once in the genus *Quadrulella*, which biomineralizes its own silica scales and once in *Hyalosphenia*, which builds entirely proteinaceous scales without mineral parts. In the scenario of ~~(Oliverio et al., 2014)~~, kleptosquamy is lost 3 times because the genus *Hyalosphenia* is not monophyletic. The non-monophyly of *Hyalosphenia* has no effect on the ancestral character state for hyalosphenids as a whole (Figure 5).

Molecular clock reconstructions

To determine the origin of hyalosphenids, we generated a dated tree for the arcellinids (**Figure 6, left**). In order to do so, we used the previously established opisthokont calibration points and a conservative calibration point for the minimum date of origin of the Arcellinida – this calibration point is used conservatively as calibrating the entire Arcellinida, as opposed to the less inclusive family Arcellidae as suggested by affinities in the original description (Porter, Meisterfeld & Knoll, 2003). In this reconstruction, we used the uncorrelated gamma multipliers model for the distribution of divergence times. This is because in our model fit analyses, this model yielded the largest Bayes Factor (logBF interval of 18.7-26.9, against 12.8-14.5 for CIR model and 16.6-24.7 for lognormal model). The Bayes Factor is one of many proposed methods to measure the appropriateness of a given model for the data at hand, and a larger BF indicates a better model fit (Lartillot & Philippe, 2006). Hence, all results discussed are based on that model. The reconstruction ran for circa 55,000 cycles until convergence between the two chains was achieved.

Our reconstruction stands in sharp contrast with another recent molecular clock reconstruction of the arcellinids (Fiz-Palacios, Leander & Heger, 2014). The two most likely reasons for this are: 1) although Fiz-Palacios and colleagues used a part of the same dataset used here, we focused on the SSU rDNA partition and not on the protein coding partition; 2) we included mostly opisthokont fossils as calibration points, but Fiz-Palacios and colleagues used a number of Meso- and Cenozoic microfossils as calibration points for internal families of arcellinids. To test the influence of these hypotheses, we implemented the calibration points suggested by Fiz-Palacios in our framework. This yielded an additional tree (**Figure 6, right**). This tree is very similar to the tree obtained by Fiz-Palacios and colleagues, with all origins of groups tending to appear at younger dates. For instance, the origin of arcellinids as a whole shifts from 944 mya to 600 mya using the Meso- and Cenozoic fossils. This is representative of a general trend throughout the tree. Therefore, the distinct dates obtained in the reconstruction presented in ~~Figure 5, left do~~ not stem from focusing on the SSU rDNA partition, but rather from the use of distinct calibration points. Hence, the interpretation of fossils is paramount in defining which result is more likely to reconstruct the actual history of Arcellinida.

Discussion

Kleptosquamy can be inferred as an ancestral character state in hyalosphenids (Figure 5), i.e., the last common ancestor of all extant hyalosphenids was able to re-use euglyphid scales. Hyalosphenid biology is not well understood, because most attempts to culture these organisms have failed. Strains that have been maintained for a certain time (*Nebela collaris*) had to be fed with fast-growing species of euglyphids, such as *Euglypha hyalina* (Ralf Meisterfeld, personal communication). For instance, one cannot say with certainty whether a hyalosphenid is able to construct the shell without any euglyphid scales. This caveat undermines the interpretation of klepstosquamy as ancestral in the group, for this reason, we clearly establish that our *working* hypothesis is that scaled euglyphids appeared before

hyalosphenids.

The fossil record of euglyphids is quite sparse and does not currently allow accurate timing of their evolution. The very well documented microfossils of *Scutiglypha* from diatomaceous earth demonstrate that modern genera have existed for at least 15 million years (Foissner & Schiller, 2001). More recently, Eocene microfossils have unambiguously pushed the fossil record of euglyphids back to 50 million years ago (Barber, Siver & Karis, 2013), including members of the genus *Scutiglypha* (Euglyphidae). Older records of shells are much more difficult to interpret, as the conditions of shell preservation make the separation between arcellinids and euglyphids ever more difficult: because of intense convergence, pseudopods would be the only reliable way of separating arcellinids and euglyphids, but these are usually not preserved in the fossil record (Bosak et al., 2011; Lahr et al., 2014). For instance, some vase shaped microfossils described from the Chuar group, especially *Melicerion poikilon*, *Bonniea* spp. and *Bombycion micron* have morphological characteristics that are compatible with euglyphid testate amoebae: the typical vase shape, thin walls, terminal aperture, homogeneously shaped and sized scales and an apparent siliceous composition. However, an arcellinid origin cannot be excluded, *Quadrulella*, a modern arcellinid, shares all those features (Porter & Knoll, 2000; Porter, Meisterfeld & Knoll, 2003). Hence, new discoveries of exceptionally preserved and properly described arcellinid and euglyphid fossils are necessary to inform interpretations of origin and diversification (Bosak et al., 2011; Dalton et al., 2013; Fiz-Palacios, Leander & Heger, 2014; Strauss et al., 2014).

The dated reconstruction presented here uses a single-locus and external calibration points to the arcellinids and places the origin of hyalosphenids in the Paleozoic (about 370 mya, with a 95% confidence interval that extends from the Neoproterozoic to Triassic). This is in marked contrast to the recent reconstruction of arcellinid history by Fiz-Palacios and colleagues (~~Fiz-Palacios, Leander & Heger,~~ 2014), which placed the origin of hyalosphenids in the

Cretaceous, about 130 mya (with a 95% confidence interval between the Devonian and the Eocene). These authors used a very similar dataset, but included both the SSU rDNA and five additional protein coding genes (both analyses are based on the dataset published by ~~Lahr and colleagues (2013)~~). The 240 million year difference between the two reconstructions is significant and may lead to very distinct implications. The use of the same calibration points as Fiz-Palacios and colleagues, combined with our search strategy, produced a tree that is very similar to the results of Fiz-Palacios et al. and estimate a Cretaceous rise of hyalospheniids. The additional calibration points used are controversial, some are based on fossils whose descriptions have not clearly established syngenicity with the matrix and may be contaminants (Farooqui et al., 2010; Kumar, 2011); others come from amber and the identity of organisms is established using optical microscopy alone (Schmidt, Schönborn & Schäfer, 2004; Schmidt et al., 2006; Girard et al., 2011). The inclusion of these fossils as calibration points led to an interesting scenario interpreted by Fiz-Palacios et al. (2014): that hyalosphenids are an ancient lineage that diversified when the complex peatland environments became available. The caveat is that many aspects of the identities of fossils used as calibration points remain to be clarified – this does not mean that the interpretations are incorrect.

The new molecular clock reconstruction (**Figure 6**) suggests that various testate amoebae including hyalospheniids, the aquatic *Arcella* + *Netzelia* clade, as well as the soil dwelling *Trigonopyxis* + *Bullinularia* clade have diversified after mid-Devonian. In contrast to the preceding periods, when plant cover was restricted to moist habitats, the Late Devonian and the Carboniferous saw the diversification of plants that were well adapted to life on land, with deeper roots and soil forming capabilities (e.g., (Gibling & Davies, 2012; Kenrick et al., 2012)). These plants formed extensive forests, established their own, humid environments, and produced abundant organic matter as well as soils (Kenrick et al., 2012), matching the appearance of the *Bullinularia* clade. These evolutionary events likely influenced the Si cycling

311 on land as well due to two main factors: 1) The root systems of the Late
312 Devonian/Carboniferous plants are thought to have promoted silicate weathering (e.g., (Algeo,
313 Scheckler & Maynard, 2001)), and 2) Tree-like Lycopodiophyta, Equisetales and liverworts,
314 plants whose modern relatives can accumulate as much or more Si than grasses (Hodson et al.,
315 2005), were abundant in forest ecosystems. Our new molecular clock reconstruction and the
316 coinciding sequence of evolutionary and ecological changes that have been documented in the
317 fossil record inspire questions. Did the release of Si from plants and the accumulation of Si in
318 the plates of biomineralizing testate amoebae as well as in various predatory species strengthen
319 the links between the C and the Si cycles on land? The annual rate of biosilification by testate
320 amoebae was shown to be of the same order as the uptake rate by trees (Aoki, Hoshino &
321 Matsubara, 2007; M. Sommer, 2012; Puppe et al., 2014) and the size of the Si pool in testate
322 amoebae increases with vegetation development in some early ecosystem successions (Puppe
323 et al., 2014).

324 To move forward from here we need to i) better understand Si metabolism across protist
325 groups, including deeper understanding of physiological aspects; ii) obtain reliable fossil
326 evidence for the appearance and diversification of Si-metabolizing lineages; iii) improve the
327 molecular clock by expanding the molecular database, using appropriate numerical models and
328 carefully checking the reliability of the fossil record, iv) improve constraints on the contribution of
329 Si-precipitating organisms to the cycling of Si and C in terrestrial systems. The combination of
330 these efforts is challenging, but can be met with a combination of approaches including
331 molecular phylogeny, biogeochemistry, and paleontology.

332 **Data accessibility**

333 Alignments and phylobayes runs will be made available upon acceptance of the article.

Acknowledgments

We are thankful for the associate editor as well as two reviewers for relevant criticism of the manuscript

337 References

338 Alexandre A., Meunier J-D., Colin F., Koud J-M. 1997. Plant impact on the biogeochemical
339 cycle of silicon and related weathering processes. *Geochimica et Cosmochimica Acta*
340 61:677–682.
341 Algeo TJ., Scheckler SE., Maynard JB. 2001. Effects of the Middle to Late Devonian spread of
342 vascular land plants on weathering regimes, marine biotas, and global climate. *Plants*
343 *invade the land: Evolutionary and environmental perspectives*:213–236.
344 Anderson OR. 1987. Fine Structure of a Silica-Biomineralizing Testate Amoeba, *Netzelia*
345 *tuberculata*. *The Journal of Protozoology* 34:302–309.
346 Anderson OR. 1989. Some observations of feeding behavior, growth, and test particle
347 morphology of a silica-secreting testate amoeba *Netzelia tuberculata* (Wallich)
348 (Rhizopoda, Testacea) grown in laboratory culture. *Archiv für Protistenkunde* 137:211–
349 221.
350 Anderson OR. 1994. Cytoplasmic origin and surface deposition of siliceous structures in
351 Sarcodina. *Protoplasma* 181:61–77.
352 Aoki Y., Hoshino M., Matsubara T. 2007. Silica and testate amoebae in a soil under pine–oak
353 forest. *Geoderma* 142:29–35.
354 Barber A., Siver PA., Karis W. 2013. Euglyphid Testate Amoebae (Rhizaria: Euglyphida) from
355 an Arctic Eocene Waterbody: Evidence of Evolutionary Stasis in Plate Morphology For
356 Over 40 Million Years. *Protist* 164:541–555.
357 Benton MJ., Donoghue PC., Asher RJ., Friedman M., Near TJ., Vinther J. 2015. Constraints on
358 the timescale of animal evolutionary history. *Palaeontologia Electronica* 18:1–106.
359 Bosak T., Lahr DJG., Pruss SB., Macdonald FA., Dalton L., Matys E. 2011. Agglutinated tests in
360 post-Sturtian cap carbonates of Namibia and Mongolia. *Earth and Planetary Science*

Letters 308:29–40.

Cary L., Alexandre A., Meunier J-D., Boeglin J-L., Braun J-J. 2005. Contribution of phytoliths to the suspended load of biogenic silica in the Nyong basin rivers (Cameroon). *Biogeochemistry* 74:101–114.

Châtelet EA du., Noiriel C., Delaine M. 2013. Three-Dimensional Morphological and Mineralogical Characterization of Testate Amebae. *Microscopy and Microanalysis* 19:1511–1522.

Conley DJ. 2002. Terrestrial ecosystems and the global biogeochemical silica cycle. *Global Biogeochemical Cycles* 16:68–1.

Cornelis J-T., Delvaux B., Georg RB., Lucas Y., Ranger J., Opfergelt S. 2011. Tracing the origin of dissolved silicon transferred from various soil-plant systems towards rivers: a review. *Biogeosciences* 8:89–112.

Dalton LA., Bosak T., Macdonald FA., Lahr DJG., Pruss SB. 2013. Preservational and Morphological Variability of Assemblages of Agglutinated Eukaryotes in Cryogenian Cap Carbonates of Northern Namibia. *PALAIOS* 28:67–79.

Deflandre G. 1936. Etude monographique sur le genre Nebela Leidy. *Ann Protistol* 5:201–286.

Donoghue PC., Benton MJ. 2007. Rocks and clocks: calibrating the Tree of Life using fossils and molecules. *Trends in Ecology & Evolution* 22:424–431.

Douglas MSV., Smol JP. 2001. Siliceous Protozoan Plates and Scales. In: Smol JP, Birks HJB, Last WM, Bradley RS, Alverson K eds. *Tracking Environmental Change Using Lake Sediments*. Developments in Paleoenvironmental Research. Springer Netherlands, 265–279.

Farooqui A., Kumar A., Jha N., Pande AC., Bhattacharya DD. 2010. A Thecamoebian

384 Assemblage from the Manjir Formation (Early Permian) of Northwest Himalaya, India.
385 *E-Journal Earth Science India* 3:146–153.
386 Fiz-Palacios O., Leander BS., Heger TJ. 2014. Old Lineages in a New Ecosystem:
387 Diversification of Arcellinid Amoebae (Amoebozoa) and Peatland Mosses. *PLoS ONE*
388 9:e95238.
389 Foissner W., Schiller W. 2001. Stable for 15 million years: scanning electron microscope
390 investigation of Miocene euglyphid thecamoebians from Germany, with description of
391 the new genus Scutiglypha. *European Journal of Protistology* 37:167–180.
392 Gibling MR., Davies NS. 2012. Palaeozoic landscapes shaped by plant evolution. *Nature*
393 *Geoscience* 5:99–105.
394 Girard V., Néraudeau D., Adl SM., Breton G. 2011. Protist-like inclusions in amber, as
395 evidenced by Charentes amber. *European Journal of Protistology* 47:59–66.
396 Gomaa F., Todorov M., Heger TJ., Mitchell EAD., Lara E. 2012. SSU rRNA Phylogeny of
397 Arcellinida (Amoebozoa) Reveals that the Largest Arcellinid Genus, Difflugia Leclerc
398 1815, is not Monophyletic. *Protist* 163:389–399.
399 Gröger C., Lutz K., Brunner E. 2008. Biomolecular Self-assembly and its Relevance in Silica
400 Biomineralization. *Cell Biochemistry and Biophysics* 50:23–39.
401 Hedley DRH., Ogden CG. 1974. Adhesion plaques associated with the production of a daughter
402 cell in Euglypha (Testacea; Potozoa). *Cell and Tissue Research* 153:261–268.
403 Heger TJ., Pawlowski J., Lara E., Leander BS., Todorov M., Golemansky V., Mitchell EAD.
404 2011. Comparing Potential COI and SSU rDNA Barcodes for Assessing the Diversity
405 and Phylogenetic Relationships of Cyphoderiid Testate Amoebae (Rhizaria: Euglyphida).
406 *Protist* 162:131–141.

Hodson MJ., White PJ., Mead A., Broadley MR. 2005. Phylogenetic variation in the silicon composition of plants. *Annals of Botany* 96:1027–1046.

Karlstrom KE., Bowring SA., Dehler CM., Knoll AH., Porter SM., Des Marais DJ., Weil AB., Sharp ZD., Geissman JW., Elrick MB., others 2000. Chuar Group of the Grand Canyon: Record of breakup of Rodinia, associated change in the global carbon cycle, and ecosystem expansion by 740 Ma. *Geology* 28:619–622.

Kenrick P., Wellman CH., Schneider H., Edgecombe GD. 2012. A timeline for terrestrialization: consequences for the carbon cycle in the Palaeozoic. *Philosophical Transactions of the Royal Society of London B: Biological Sciences* 367:519–536.

Kosakyan A., Heger TJ., Leander BS., Todorov M., Mitchell EAD., Lara E. 2012. COI Barcoding of Nebelid Testate Amoebae (Amoebozoa: Arcellinida): Extensive Cryptic Diversity and Redefinition of the Hyalospheniidae Schultze. *Protist* 163:415–434.

Kumar A. 2011. Acid-resistant Cretaceous thecamoebian tests from the Arabian Peninsula: a suggestion for study of agglutinated rhizopods in palynological slides. *Journal of Micropalaeontology* 30:1–5.

Lahr DJ., Laughinghouse HD., Oliverio AM., Gao F., Katz LA. 2014. How discordant morphological and molecular evolution among microorganisms can revise our notions of biodiversity on Earth. *BioEssays* 36:950–959.

Lahr DJG., Grant JR., Katz LA. 2013. Multigene Phylogenetic Reconstruction of the Tubulinea (Amoebozoa) Corroborates Four of the Six Major Lineages, while Additionally Revealing that Shell Composition Does not Predict Phylogeny in the Arcellinida. *Protist* 164:323–339.

Lara E., Heger TJ., Ekelund F., Lamentowicz M., Mitchell EAD. 2008. Ribosomal RNA Genes

Challenge the Monophyly of the Hyalospheniidae (Amoebozoa: Arcellinida). *Protist* 159:165–176.

Lartillot N., Lepage T., Blanquart S. 2009. PhyloBayes 3: a Bayesian software package for phylogenetic reconstruction and molecular dating. *Bioinformatics* 25:2286–2288.

Lartillot N., Philippe H. 2006. Computing Bayes Factors Using Thermodynamic Integration. *Systematic Biology* 55:195–207.

Leidy J. 1879. Fresh-Water Rhizopods of North America. 12:1–327.

Maddison WP., Maddison DR. 2007. Mesquite: a modular system for evolutionary analysis. Version 2.75. 2011. *URL http://mesquiteproject. org*.

Marron AO., Alston MJ., Heavens D., Akam M., Caccamo M., Holland PWH., Walker G. 2013. A family of diatom-like silicon transporters in the siliceous loricate choanoflagellates. *Proceedings of the Royal Society B: Biological Sciences* 280:20122543.

Meisterfeld R. 2002. Order Arcellinida Kent, 1880. *The illustrated guide to the Protozoa* 2:827–860.

M. Sommer HJ. 2012. Si cycling in a forest biogeosystem - the importance of anthropogenic perturbation and induced transient state of biogenic Si pools. *Biogeosciences Discussions* 9:18865–18906.

Oliverio AM., Lahr DJ., Nguyen T., Katz LA. 2014. Cryptic Diversity within Morphospecies of Testate Amoebae (Amoebozoa: Arcellinida) in New England Bogs and Fens. *Protist*.

Parfrey LW., Lahr DJG., Knoll AH., Katz LA. 2011. Estimating the timing of early eukaryotic diversification with multigene molecular clocks. *Proceedings of the National Academy of Sciences* 108:13624–13629.

Penard E. 1902. Faune rhizopodique du bassin du Léman...

453 Porter SM., Knoll AH. 2000. Testate amoebae in the Neoproterozoic Era: evidence from vase-
454 shaped microfossils in the Chuar Group, Grand Canyon. *Paleobiology* 26:360–385.
455 Porter SM., Knoll AH. 2009. Testate amoebae in the Neoproterozoic Era: evidence from vase-
456 shaped microfossils in the Chuar Group, Grand Canyon.
457 Porter SM., Meisterfeld R., Knoll AH. 2003. Vase-Shaped Microfossils from the Neoproterozoic
458 Chuar group, Grand Canyon: a classification guided by modern testate amoebae. *Journal*
459 *of Paleontology* 77:409–429.
460 Puppe D., Kaczorek D., Wanner M., Sommer M. 2014. Dynamics and drivers of the protozoic Si
461 pool along a 10-year chronosequence of initial ecosystem states. *Ecological Engineering*
462 70:477–482.
463 Rutschmann F. 2005. Bayesian molecular dating using PAML/multidivtime. A step-by-step
464 manual. *University of Zurich*.
465 Sapriel G., Quinet M., Heijde M., Jourdren L., Tanty V., Luo G., Le Crom S., Lopez PJ. 2009.
466 Genome-Wide Transcriptome Analyses of Silicon Metabolism in Phaeodactylum
467 tricornutum Reveal the Multilevel Regulation of Silicic Acid Transporters. *PLoS ONE*
468 4:e7458.
469 Sarmiento JL. 2013. *Ocean Biogeochemical Dynamics*. Princeton University Press.
470 Schmidt AR., Ragazzi E., Coppellotti O., Roghi G. 2006. A microworld in Triassic amber.
471 *Nature* 444:835–835.
472 Schmidt AR., Schönborn W., Schäfer U. 2004. Diverse fossil amoebae in German Mesozoic
473 amber. *Palaeontology* 47:185–197.
474 Strauss JV., Rooney AD., Macdonald FA., Brandon AD., Knoll AH. 2014. 740 Ma vase-shaped
475 microfossils from Yukon, Canada: Implications for Neoproterozoic chronology and

476 biostratigraphy. *Geology*:G35736.1.

477 Thorne JL., Kishino H. 2003. Multidivtime. *Available from the authors at http://statgen. ncsu.*

478 *edu/thorne/multidivtime. html*.

479 Vucetich MC. 1974. Comentarios criticos sobre Argynnia Jung, 1942 (Rhizopoda, Testacea).

480 *Neotropica (La Plata)* 20:126–128.

481 Wilkinson DM. 2008. Testate amoebae and nutrient cycling: peering into the black box of soil

482 ecology. *Trends in ecology & evolution* 23:596–599.

483 Wilkinson DM., Mitchell EAD. 2010. Testate Amoebae and Nutrient Cycling with Particular

484 Reference to Soils. *Geomicrobiology Journal* 27:520–533.

485 Yang Z. 2007. PAML 4: Phylogenetic Analysis by Maximum Likelihood. *Molecular Biology*

486 *and Evolution* 24:1586–1591.

487

488

Figure 1(on next page)

A simplified tree of eukaryotes indicating that biomineralization is a convergent feature.

The main supergroups are indicated by the different colors and the lineages in bold contain biomineralizers. Backbone of tree is based on relationships in Katz (2012) , dotted lines represent uncertainty.

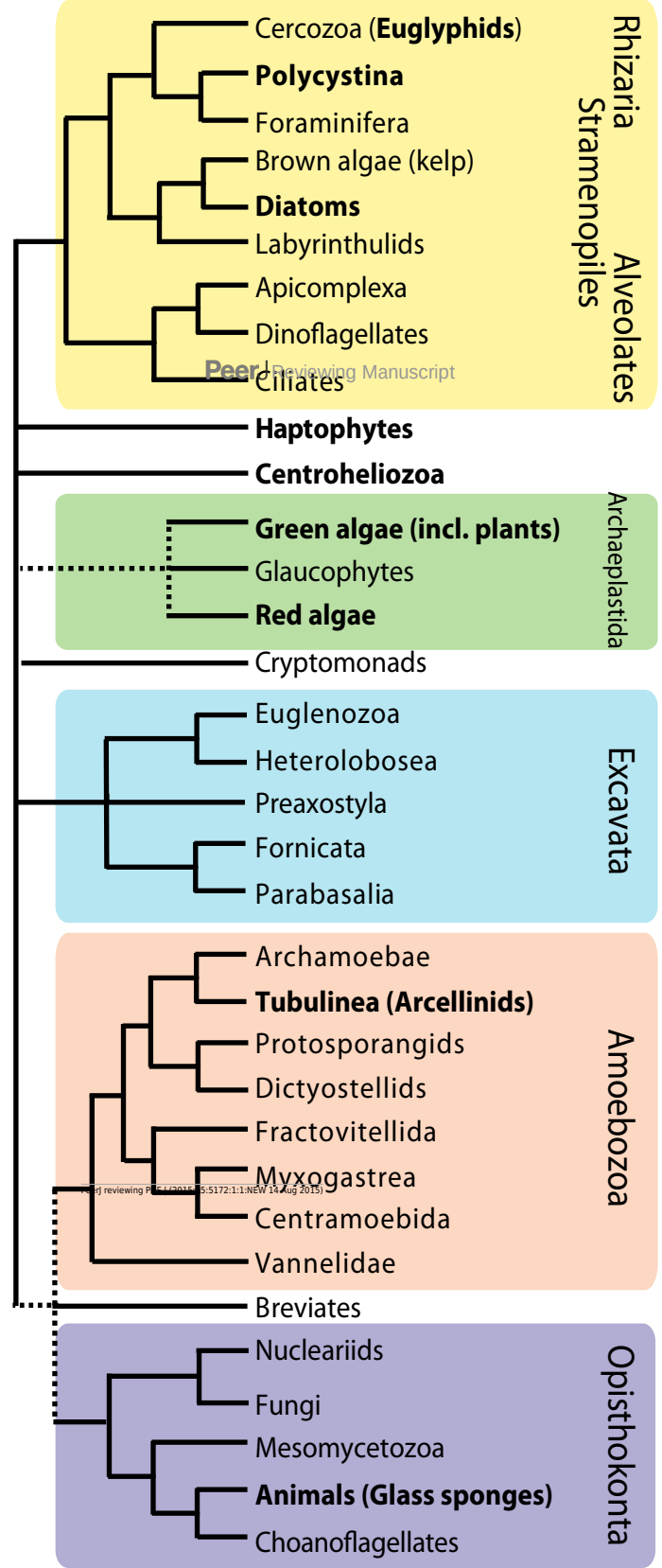

2

Examples of arcellinids shell composition.

A: *Quadrulella subcarinata* Gautier-Lièvre, 1957 constructs the shell using square particles of amorphous Si that are endogenously produced from dissolved silica (idiosomes). Specimen from *Sphagnum* collected in Welgevonden Game Park, Limpopo province, South Africa. B: *Difflugia acuminata* Ehrenberg builds its shell from agglutinated diverse particles, in this case, the organism used both centric (white arrow) and pennate (black arrow) diatom shells, along with other smaller particles. C: *Nebela marginata* Penard uses a mixture of particles with some additional biological silica deposition, such as scales scavenged from euglyphids (oval and circular plates as the one indicated by the white arrow), and pennate diatoms (black arrow). D: *Argynnia dentistoma,* this specimen has used a mixture of flat environmental mineral particles and rounded euglyphid scales to construct the shell. B-D: Specimens from Eugene Penard's collection, deposited at the Natural Museum of Geneva; photos taken by Thierry Arnet – Wikimedia document. Scale bars 30 µm.

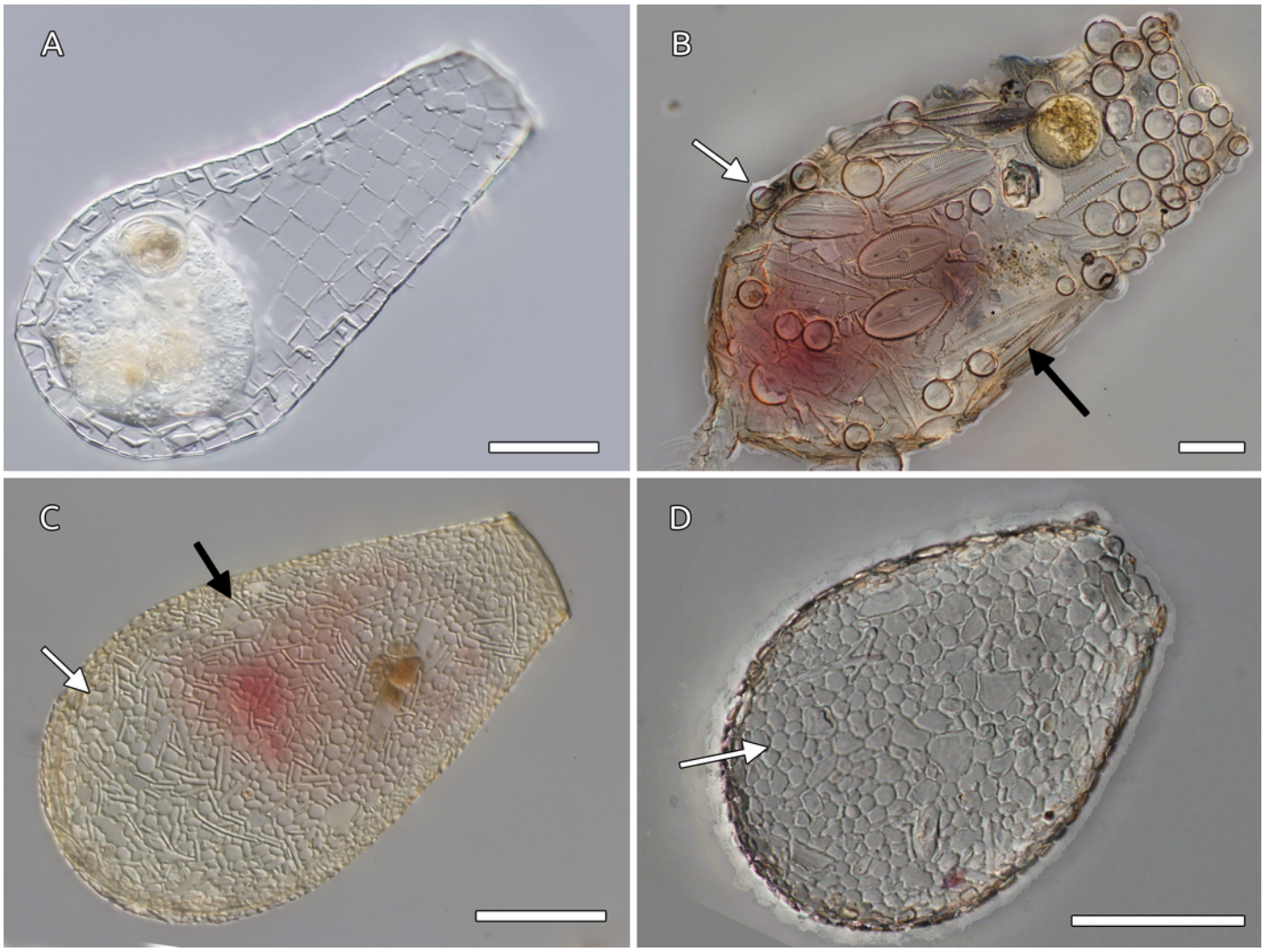
A
B
C
D

3

An example of *kleptosquamy* in the arcellinid *Apodera vas* (larger shell), obtained from predation upon the euglyphid *Sphenoderia valdiviana* (two smaller individuals).

The two species occur together in *Sphagnum magellanicum* mosses around Laguna Esmeralda, in Argentinian Tierra del Fuego. The larger scales (arrows) in the test of *A. vas* can clearly be matched to the ones produced by *S. valdiviana*.

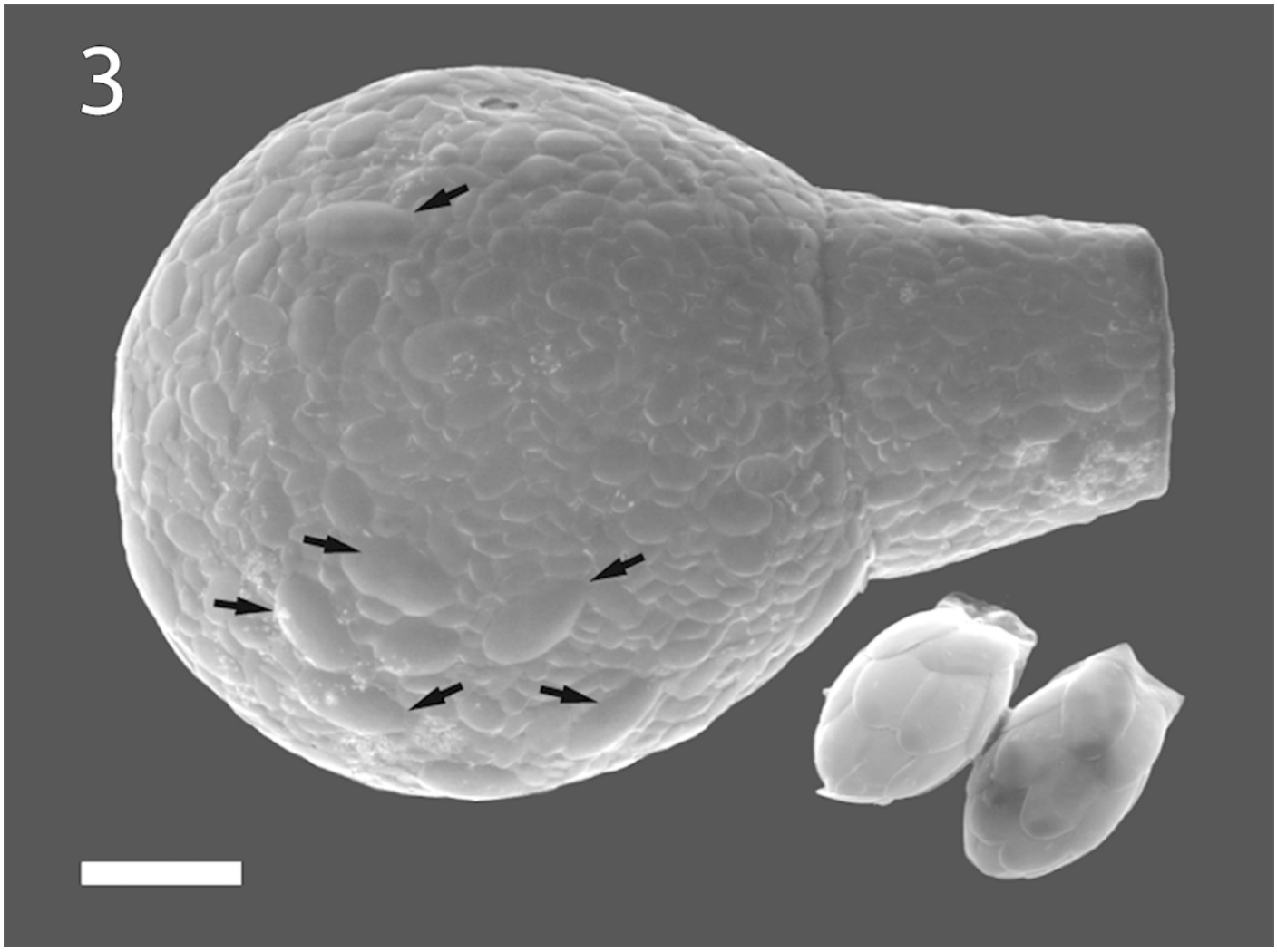

4

Kleptosquamy in *Padaungiella lageniformis*.

A: Lateral view of *P. lageniformis* ingesting cytoplasm of *Euglypha* sp., beginning of observations (T=0). B: View closer to the bottom of the plate, where the teardrop shaped apertural scales of the *Euglypha* individual are visible (white arrow), and other already ingested plates are in *P. lageniformis* cytoplasm (black arrow, T=22 min). C: A distinct optical section from B, showing a region in the *Euglypha* shell where the roughly hexagonal body plates (white arrow) were removed by the *P. lageniformis*, note that here the apertural scales are not present on this side (T=22min). D: Accumulation of plates from *Euglypha* in the cytoplasmic region of *P. lageniformis* close to the aperture (black arrows), in the cytoplasm, plates are easily when in profile view (T=22min). E: Early stage of apertural plug construction, the *P. lageniformis* has laid down two scales (black arrow) in a parallel orientation to the aperture (T=23 min). F: The organism begins to add other debris to the plug (black arrow, t=24min). G: Debris particles had been added to the plug, notice vesicles of yellowish-brown material in the cytoplasm (black arrows), these are later added to the plug (T=1h13min). H: Yellowish-brown debris moves closer to the aperture (black arrows, T=1h 13min). I: All debris particles finally added to the apertural plug (black arrows, T=1h32min). J: After apertural plug is finished, the cell goes into a cyst (T=1h52min). K: Whole view of digestive cyst (T=1h52min). L: Emergence of cyst 12 hours later, many scales are visible in the cytoplasm (black arrows), they were recollected from the plug. Other types of particles were discarded. Scale bar = 20µm (B-J) and 50µm (A, K, L).

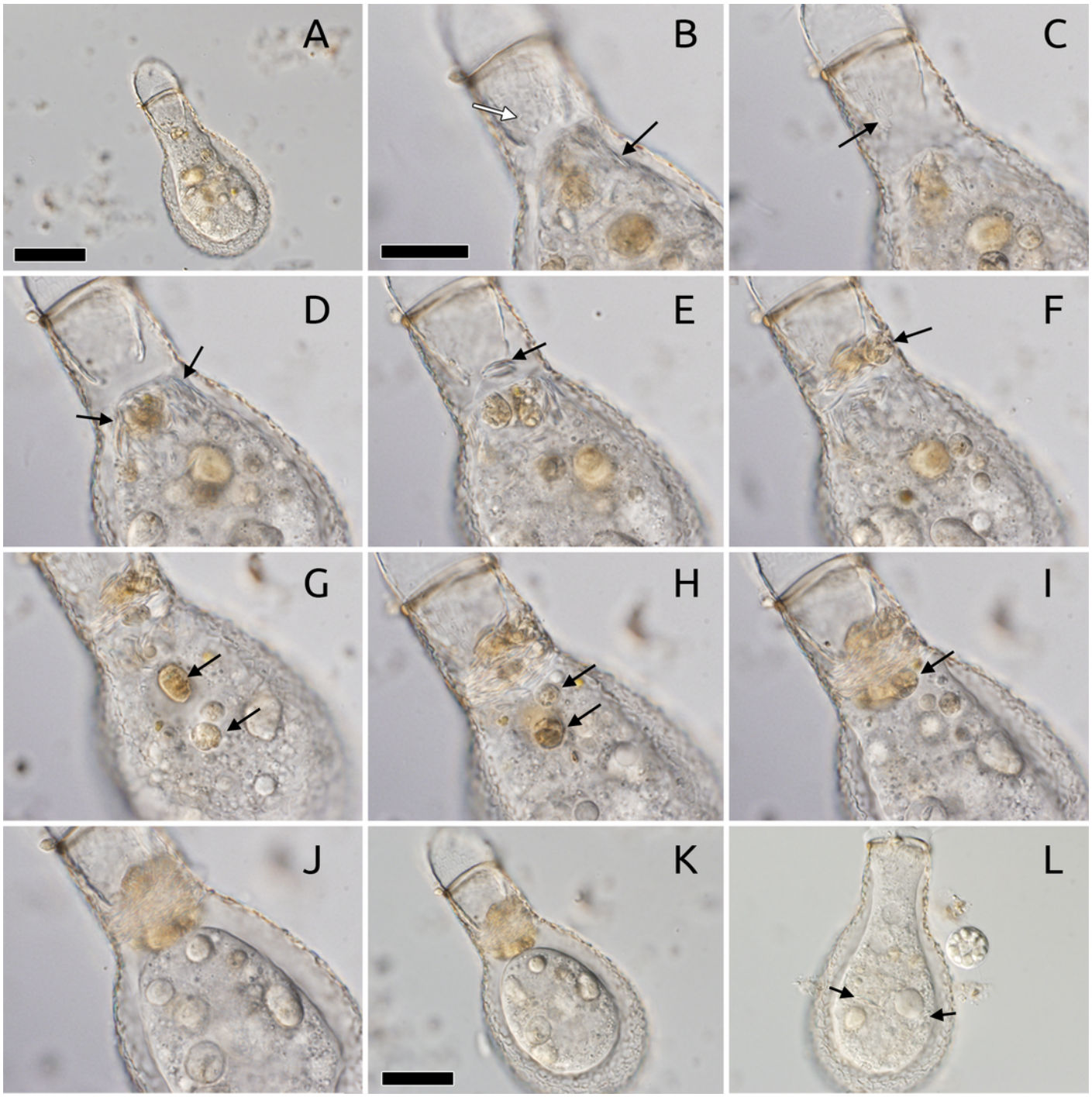
A
B
C
D
E
F
G
H
I
J
K
L

5

Evidence of kleptosquamy in other hyalosphenid genera.

A: A specimen of *Porosia bigibbosa* in a digestive cyst, with an apertural plug constructed partly with siliceous scales (white arrows). Specimen from mosses collected on an erratic boulder near the Merdasson river, Neuchâtel, Switzerland. B: A specimen of *Nebela marginata*, about to enter the digestive cyst, presenting also an apertural plug constructed with a layer of siliceous scales (white arrows), among others. Specimen from *Sphagnum* collected in Les Pontin bog, Canton Bern, Switzerland. Scale bar = 50µm.

Figure 6(on next page)

Ancestral state reconstruction of kleptosquamy in the hyalosphenid genera.

The backbone of each cladogram is one of two most current hyalosphenid phylogenies, based on distinct sets of genes. Colors along the tree branches represent how states changed through evolution for this character.

a) Kosakyan et al. (Cox 1)

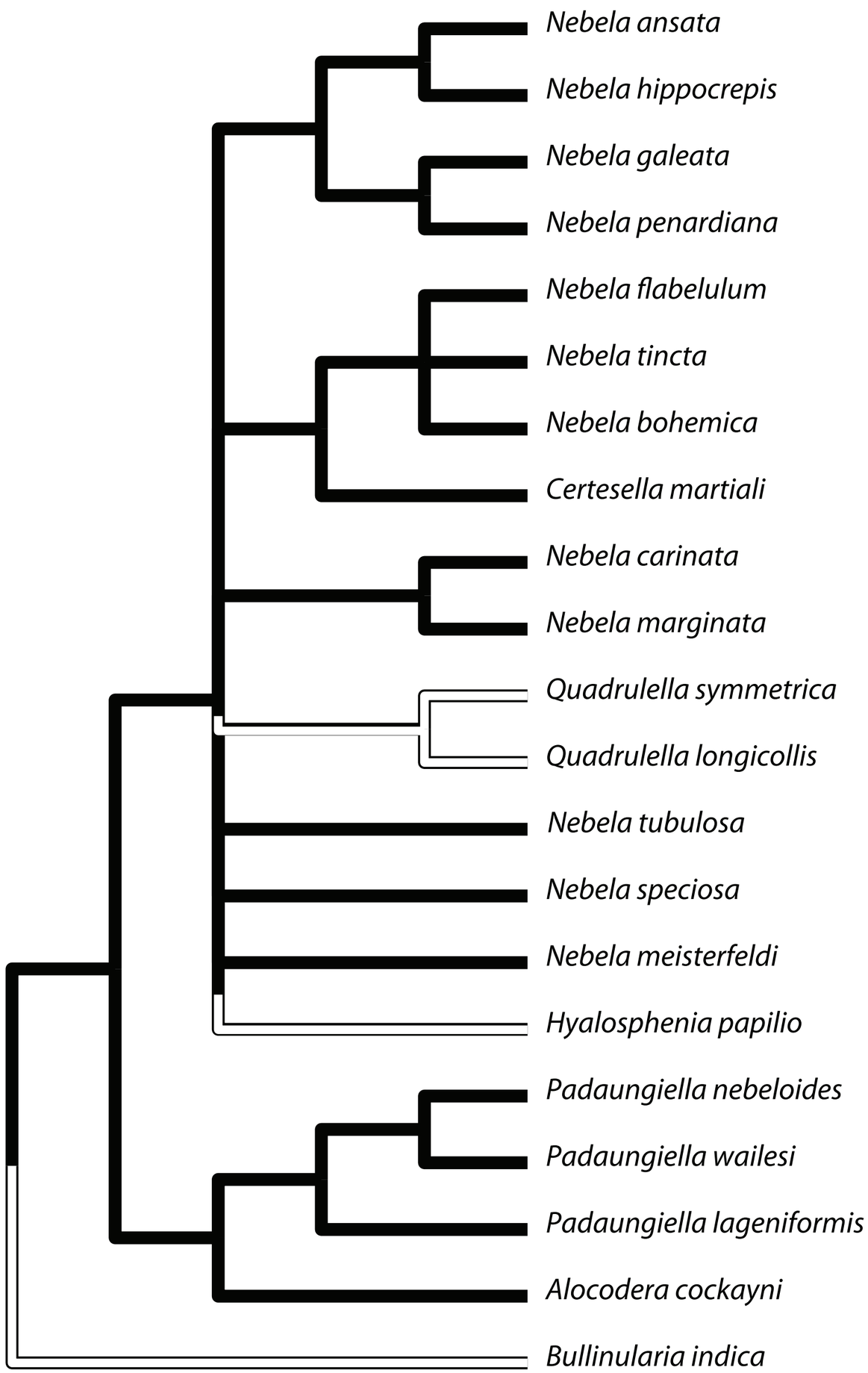

b) Oliverio et al. (SSU rDNA)

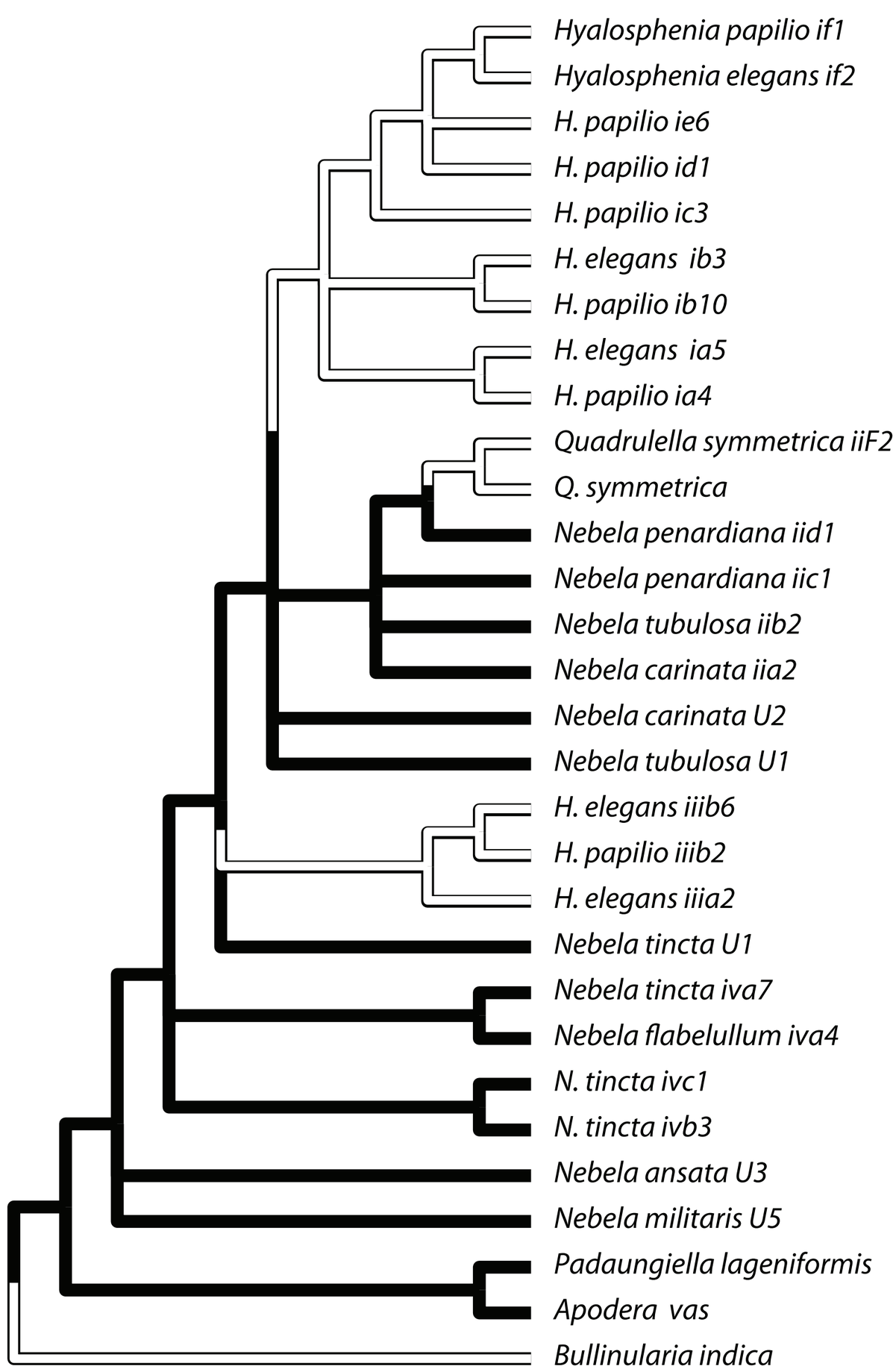

kleptosquamy present

kleptosquamy absent

Figure 7 (on next page)

Comparison between dated phylogenies of Arcellinida based on molecular clock reconstructions using distinct sets of calibration points.

Both reconstructions were based on a 109 taxon, 914 positions alignment. Taxa that are not relevant for the present discussion have been collapsed for clarity. The reconstruction on the left uses a single arcellinid calibration point (indicated), and other 5 calibration points inside the Opisthokonta. The reconstruction on the right uses the previous 6 calibration points plus 3 additional arcellinid calibration points. Although the mean value for node times can be quite different, both reconstructions are within the 95% confidence interval of each other (indicated by blue bars).

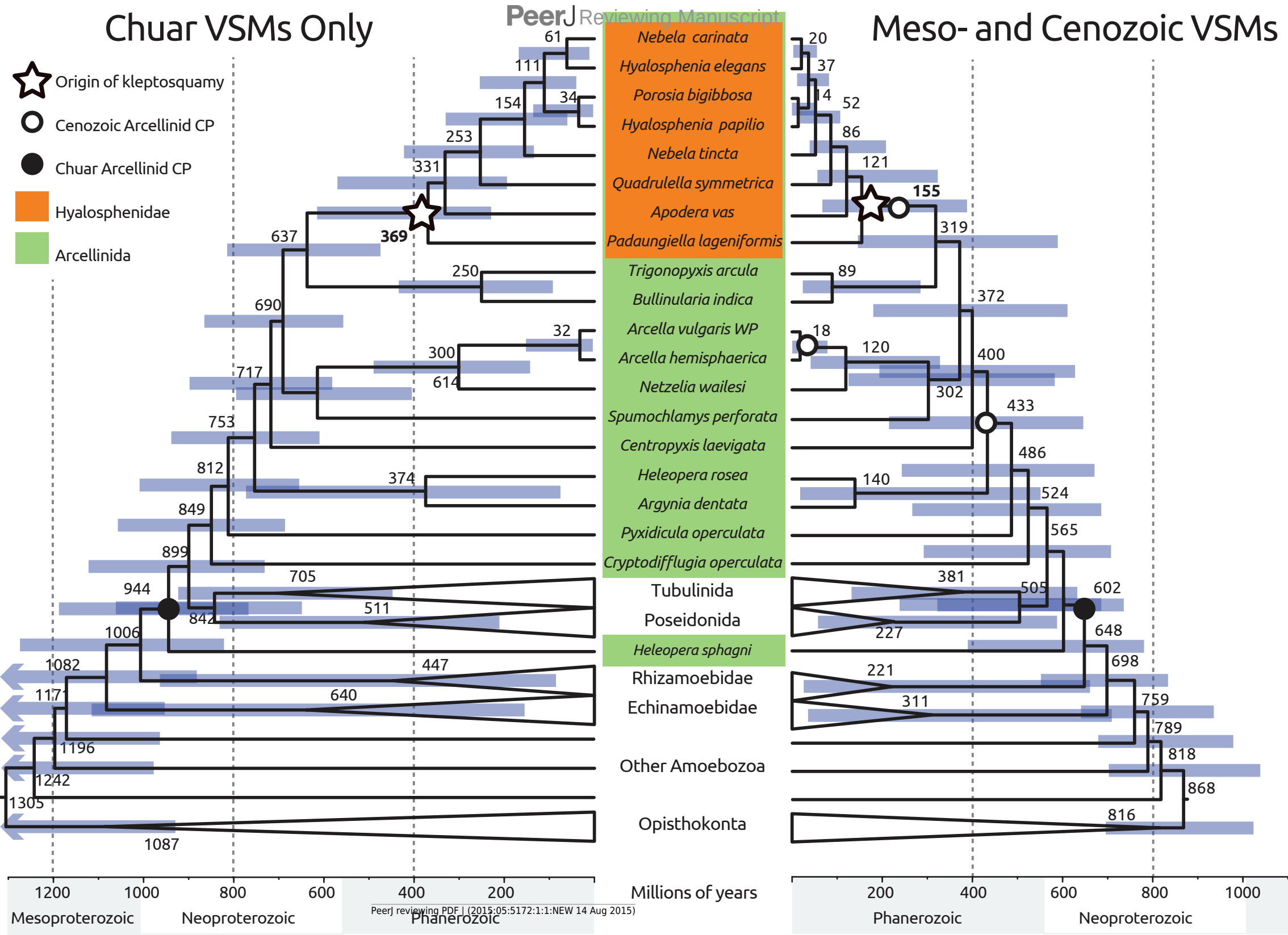

Table 1(on next page)

Summary of calibration points used of molecular clock reconstructions. Dates are in millions of years.

Table 1: Summary of calibration points used of molecular clock reconstructions. Dates are in millions of years.

Clade	Fossil	Taxa used for delimitation	Max date	Min date
Amniota	*Westlonthiana*	*Gallus gallus* and *Homo sapiens*	400	328.3
Ascomycetes	*Paleopyrenomycetes*	*S.s pombe* and *P. chrysosporium*	1000	400
Endopterygota	Mecoptera	*A. mellifera* and *D. melanogaster*	350	284.4
Animals	sponge biomarkers	*O. carmella* and *C. capitata*	3,000	632
Bilateria	*Kimberella*	*B. floridae* and *C. capitata*	630	555
Vertebrates	*Haikouichthys*	*B. floridae* and *H. sapiens*	555	520
Arcellinida	*Paleoarcella*	*A. hemisphaerica* and *H. sphagni*	3,000	736